Available online at www.sciencedirect.com
ScienceDirect
Ceramics International 38 (2012) 861–865
CERAMICS INTERNATIONAL
www.elsevier.com/locate/ceramint

Short communication

Synthesis of lamellar niobic acid nanorods via proton-exchange and their conversion to T-Nb_2O_5 nanorods

C.Y. Xu [a,b], Y.Z. Liu [b], L. Zhen [a,*]

[a] School of Materials Science and Engineering, Harbin Institute of Technology, 92 West Dazhi Street, Harbin 150001, China
[b] School of Materials Science and Engineering, Georgia Institute of Technology, Atlanta, GA 30332, USA

Received 24 May 2011; received in revised form 8 June 2011; accepted 27 June 2011
Available online 2nd July 2011

Abstract

We report the topochemical synthesis of lamellar niobic acid ($H_2Nb_2O_6$) nanorods via proton-exchange from single-crystal $CaNb_2O_6$ nanorods with layered structure. The obtained $H_2Nb_2O_6$ nanorods were then converted to T-Nb_2O_5 nanorods with a pseudo-hexagonal structure by thermal treatment in air. The one-dimensional characteristic of the $CaNb_2O_6$ nanorods remained during their transformation to $H_2Nb_2O_6$ and then to T-Nb_2O_5 nanorods. The structure transformation during the formation of T-Nb_2O_5 nanorods was investigated in detail using high-resolution transmission electron microscopy, and the results show that polycrystalline Nb_2O_5 nanorods were formed although the one-dimensional characteristic was well retained. The existence of texturing as well as dislocations in T-Nb_2O_5 nanorods was revealed.

Keywords: Electron microscopy; Nanostructures; Layered compounds

1. Introduction

Lamellar solid acids containing titanium and niobium (e.g., $H_2Ti_4O_9$, HNb_3O_8 and $H_4Nb_6O_{17}$) are promising photocatalysts for their several unique characteristics, for example, the valence band top and the conduction band bottom are located at deserved potential levels, the layered structure facilitates electron transfer, and the protonic acidity is favorable for water and some organic molecules absorption [1,2]. Several protonated compounds have been proved to show higher photocatalytic activities for hydrogen generation from water splitting than their corresponding salt phases under UV light [3–5]. The layered materials can be also exfoliated chemically to prepare unlamellar colloids that possess interesting possibility of restacking by scrolling into tubulars structures [6,7]. In addition, the lamellar solid acids can be served as precursors to prepare binary oxide nanocrystals through dehydration. For example, Bruce and co-workers reported the formation of hydrogen titanate nanowires, which were converted to TiO_2-B nanowires by subsequent annealing [8].

Niobium pentoxide (Nb_2O_5) is an important *n*-type semiconductor with a wide band gap of about 3.4 eV, and has shown many remarkable applications in gas sensors, catalysts, optical and electrochromic devices [9–12]. The chemical and physical properties of micro- and nanostructured metal oxide semiconductors have close relationship with their morphologies [13–15]. Recently, much attention has been paid to the preparation of Nb_2O_5 one-dimensional (1D) nanostructures as well as its hierarchical micro- and nanostructures. Mozetič et al. first reported the synthesis of Nb_2O_5 nanowires grown on Nb foils via cold plasma treatment using a high neutral oxygen flux [16]. Vertically oriented Nb_2O_5 nanowires on Nb foils were synthesized by a thermal oxidation method, and the nanowires field-emission emitters show fairly low turn-on and threshold field and high current density [17]. Mallouk and co-workers [7] proposed a scrolled sheet precursor route to polycrystalline niobium oxide nanotubes via dehydration of $H_4Nb_6O_{17}{\cdot}4H_2O$ scrolls, which were prepared by exfoliation of $K_4Nb_6O_{17}$ with layered structure. Single-crystal Nb_2O_5 nanobelts were synthesized by thermal treatment of layered structure $NH_4Nb_3O_8$ nanobelts, and the photovoltaic performance of dye-sensitized solar cells using the Nb_2O_5 nanobelts as electrode material was investigated [18]. Xue et al. [19,20] reported the formation of monoclinic Nb_2O_5 nanotube arrays

* Corresponding author. Tel.: +86 451 8641 2133; fax: +86 451 8641 3922.
E-mail address: lzhen@hit.edu.cn (L. Zhen).

0272-8842/$36.00
doi:10.1016/j.ceramint.2011.06.054

through phase transformation from pseudo-hexagonal Nb_2O_5 nanotube arrays accompanied by void formation. They also prepared Nb_2O_5 hollow microspheres and 3D superstructures via simple solution route [21–23].

In this paper, we report the synthesis of a lamellar solid acid of $H_2Nb_2O_6$ nanorods via proton-exchange from layered $CaNb_2O_6$ nanorods. The obtained $H_2Nb_2O_6$ nanorods were then converted to T-Nb_2O_5 nanorods by thermal treatment in air, which was proven to be an effective strategy for the fabrication of porous structures [24]. The structure of the obtained T-Nb_2O_5 nanorods was characterized, and the transformation process was discussed.

2. Experimental

The precursor $CaNb_2O_6$ nanorods were synthesized via molten-salt ion-exchange route, which was reported in our early work [25]. The obtained $CaNb_2O_6$ nanorods were single-crystal in nature with a preferential growth direction along [0 0 1] crystallographic direction. Proton-exchange was performed at room temperature upon acid washing for 30 min using 3 M HCl aimed by ultrasonication, resulting in the formation of $H_2Nb_2O_6$ nanorods. T-Nb_2O_5 nanorods were obtained by annealing $H_2Nb_2O_6$ nanorods at 700 °C for 3 h. The transformation process is described as follow:

$$CaNb_2O_6 + 2HCl \rightarrow H_2Nb_2O_6 + CaCl_2 \quad (1)$$

$$H_2Nb_2O_2 \xrightarrow{700\,^{\circ}C,\ 3\,h} \text{T-}Nb_2O_5 \quad (2)$$

The morphology of the obtained nanorods was examined by field-emission scanning electron microscope (SEM, LEO 1530) equipped with energy-dispersive X-ray spectroscopy (EDS). X-ray diffraction (XRD) pattern was collected using Philips X'pert diffractometer with high-intensity Cu K_α irradiation

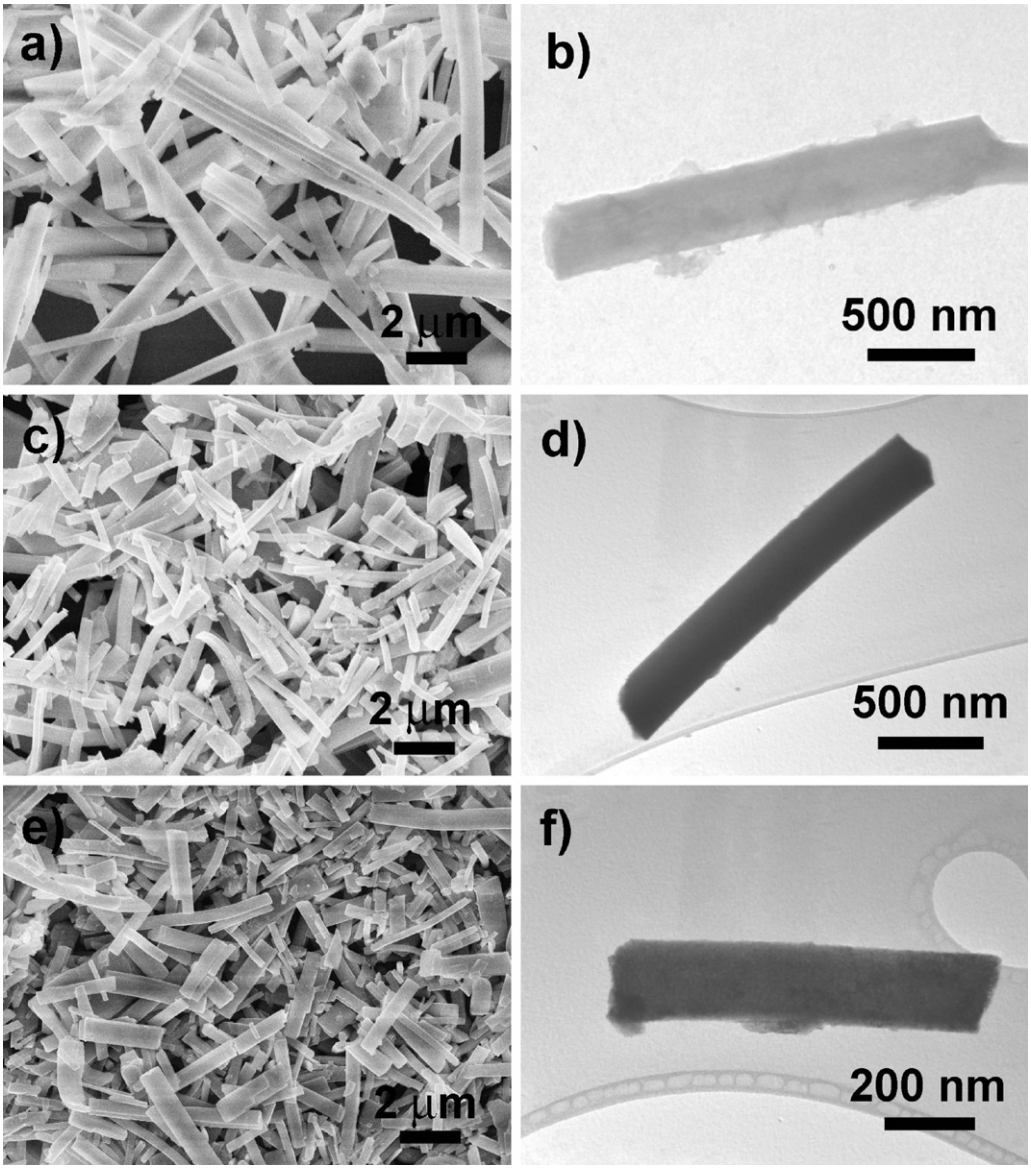

Fig. 1. (a, c, and e) SEM images of $CaNb_2O_6$, $H_2Nb_2O_6$ and T-Nb_2O_5 nanorods, respectively, showing the 1D morphology consistence during the structure transformation. (b, d, and f) Typical TEM images of $CaNb_2O_6$, $H_2Nb_2O_6$ and T-Nb_2O_5 nanorods, respectively.

(λ = 1.5406 Å). Transmission electron microscope (TEM) observation was carried out on a JEM 100CX microscope, and high-resolution transmission electron microscopy (HRTEM) experiments were conducted on a JEM 4000EX microscope.

3. Results and discussion

The morphology of the precursor $CaNb_2O_6$ nanorods was examined by SEM, as shown in Fig. 1a. The diameters of $CaNb_2O_6$ nanorods are in the range of 200 nm to 1 μm, and the lengths can reach up to 10 μm. Fig. 1b shows a typical TEM image of a single $CaNb_2O_6$ nanorod with a diameter of about 400 nm. The precursor nanorods of $CaNb_2O_6$ prepared via a molten-salt ion-exchange method are single-crystal, with a growth direction along [0 0 1] crystallographic direction [25]. The columbite structured $CaNb_2O_6$ has a layered structure, which makes it an ideal precursor for proton-exchange. The proton exchange of $CaNb_2O_6$ nanorods leads to the formation of $H_2Nb_2O_6$ nanorods. It should be noted that the ion-exchange process could be finished within 30 min. The EDX spectrum in Fig. 2a suggests the completion of proton exchange between $CaNb_2O_6$ and $H_2Nb_2O_6$. The signal of Si element is from the Si substrate used for SEM observation. The fast ion-exchange process is thought to be associated with the layered structure of $CaNb_2O_6$, which allows the fast exchange between Ca ions and H ions. The nanorods' 1D characteristic remains unchanged after proton exchange, as depicted in Fig. 1c and d, except that the lengths of $H_2Nb_2O_6$ nanorods seem to decrease slightly. Electron diffraction analyses show that $H_2Nb_2O_6$ nanorods are amorphous. T-Nb_2O_5 nanorods were obtained by annealing $H_2Nb_2O_6$ nanorods at 700 °C for 3 h. SEM and TEM images of the obtained T-Nb_2O_5 nanorods were shown in Fig. 1e and f, respectively. The nanorods' 1D characteristic also remains unchanged after the dehydration of $H_2Nb_2O_6$ nanorods.

XRD patterns of $H_2Nb_2O_6$ and T-Nb_2O_5 nanorods are shown in Fig. 2b. Broad peaks between 20 and 35° are observed for

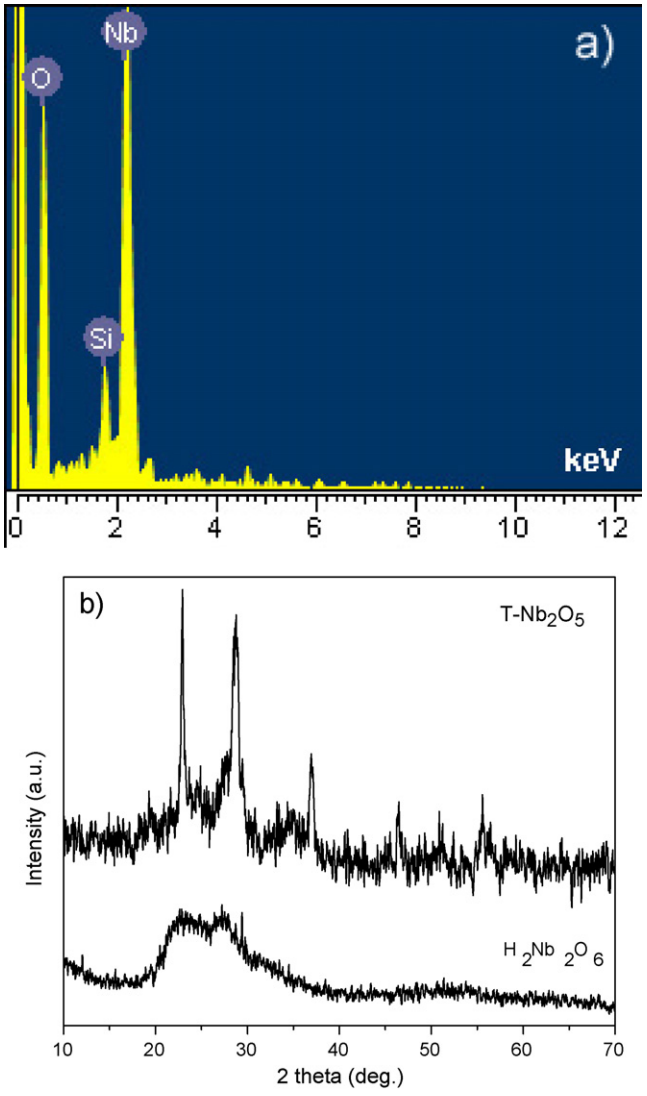

Fig. 2. (a) EDX spectrum of $H_2Nb_2O_6$ nanorods. (b) XRD patterns of $H_2Nb_2O_6$ and T-Nb_2O_5 nanorods.

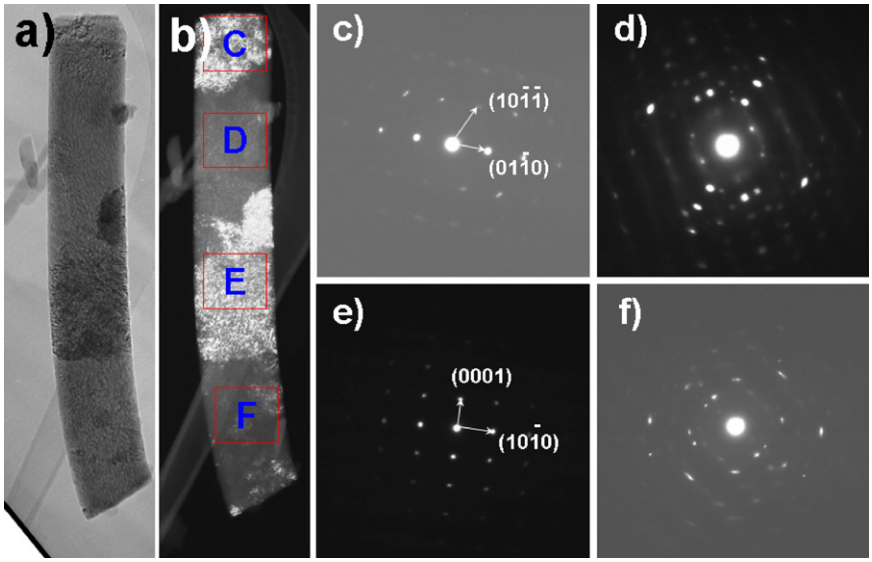

Fig. 3. (a) Bright-field and (b) corresponding dark-field TEM images of a T-Nb_2O_5 nanorod. (c–f) SAED patterns taken from different parts of the nanorod shown in (b) box-marked with C, D, E and F, respectively.

$H_2Nb_2O_6$ nanorods [2]. $H_2Nb_2O_6$ can be also written in the form of $Nb_2O_5{\cdot}H_2O$, and thus are named as niobic acid. Upon heating at 700 °C in air for 3 h, $Nb_2O_5{\cdot}H_2O$ was dehydrated and T-Nb_2O_5 was formed, as shown in Fig. 2b. T-Nb_2O_5 has a hexagonal structure [26], with lattice parameters a = 3.607 and c = 3.925 Å (PDF No. 28-0317).

The obtained T-Nb_2O_5 nanorods were further characterized by high-resolution transmission electron microscopy. Fig. 3a and b shows the bright-field and corresponding dark-field TEM images of a T-Nb_2O_5 nanorod. It is obvious that the selected nanorod is not a single-crystal, as depicted in the dark-field TEM image. Four zones with different contrasts can be indexed in Fig. 3b, which are marked with capital letters of C, D, E and F, respectively. The phenomenon is confirmed upon examination of several nanorods. Further observation found that even within one zone with the same white or dark contrast, the contrast is not uniform, and each zone consists of a wealth of fine ''particles''. Selected-area electron diffraction (SAED) patterns from the four zones are shown in panels c, d, e, and f, respectively. SAED patterns of areas C and E are from $[1\,0\,\bar{1}\,0]$ and $[01\bar{1}0]$ zone axes, respectively, while that of areas D and F are from off-axis, in which all the diffraction spots can also be indexed to T-Nb_2O_5. Slight arc-like elongation of the outer diffraction spots are observed in both Fig. 4c and e, although in which the diffraction patterns indicate the single-crystal nature of the selected areas.

High-resolution transmission electron microscopy was used to study the detailed structure of the obtained T-Nb_2O_5 nanorods produced by annealing of $H_2Nb_2O_6$ nanorods. Fig. 4 shows a noise-filtered HRTEM image from area E as indicated in Fig. 3b. The lattice image shows that the nanorod is obviously not a single-crystal nanorod, but consists of many fine *single-crystalline* particles separated by amorphous boundaries. The lattice images from these *single-crystalline* particles are from the same zone axis of $[0\,1\,\bar{1}\,0]$ without apparent deviations, and thus the diffraction pattern from a relative large zone within area E shows *single-crystal* pattern with an arc-like elongation of the outer diffraction spots, as depicted in Fig. 3e. The lattice image clearly shows the existence of texturing in the obtained Nb_2O_5 nanorods. The similar phenomena has been reported in Nb_2O_5 nanotubes derived from $H_4Nb_6O_{17}{\cdot}nH_2O$ scrolls [7]. Defects, such as dislocations, can be frequently observed in Nb_2O_5 nanorods, as marked by a white arrow in Fig. 4. The existence of dislocations decreases the mismatch energy during the structure transformation.

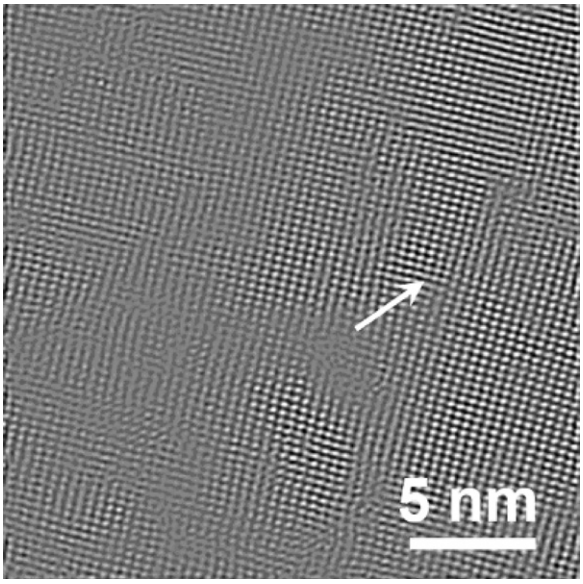

Fig. 4. FFT-filtered HRTEM image of T-Nb_2O_5 nanorods. The image was taken in area E marked in Fig. 3.

The crystal structures of $CaNb_2O_6$ and T-Nb_2O_5 are shown in Fig. 5a and b, respectively. Each layer of $CaNb_2O_6$ is composed of edge-sharing NbO_6 octahedra. Upon proton-exchange, the layer structure will not change since the diameter of H ions is much smaller than that of Ca ions. This can also explain why the proton-exchange process is rather fast. The *xy* plan of T-Nb_2O_5 is comprised of edge-sharing NbO_7 units as well as NbO_6 octahedra. These units are then

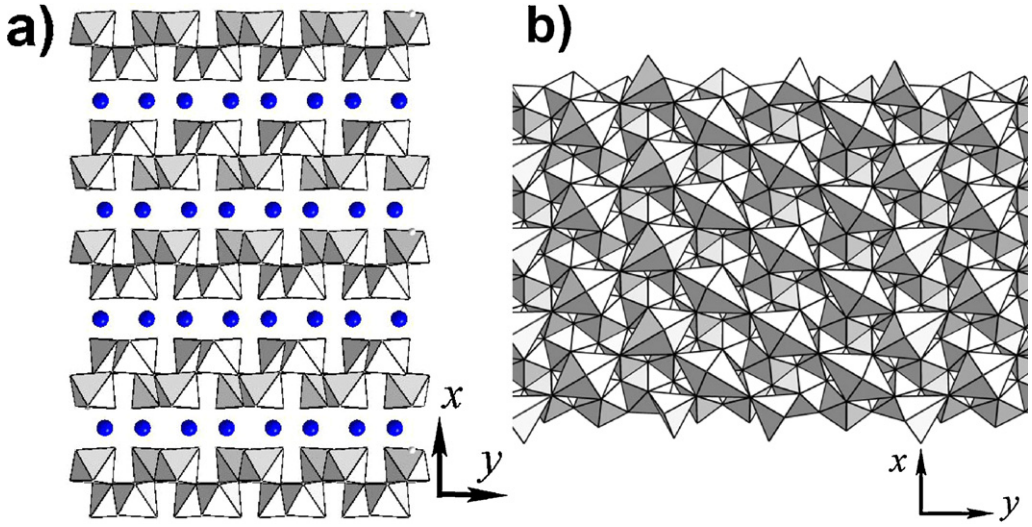

Fig. 5. Crystal structures of (a) $CaNb_2O_6$ and (b) T-Nb_2O_5.

linked by corner-sharing polyhedra along the z axis to form the three-dimensional structure [7,26]. The conversion from $H_2Nb_2O_6$ to T-Nb_2O_5 requires long-range diffusion of Nb and O atoms. Hence, it would be difficult for a single-crystal nanorod to be obtained. The slight derivation of the fine single-crystal particles from the same zone axis and the amorphous boundaries no doubt decrease the total energy.

4. Conclusions

In summary, we have demonstrated a soft chemistry route for the preparation of lamellar niobic acid nanorods, which was then converted to T-Nb_2O_5 nanorods through thermal treatment in air. The structure of the T-Nb_2O_5 nanorods was studied in detail using high-resolution transmission electron microscopy. The transformation from layered structure to pseudo-hexagonal structure results in the polycrystalline nature of T-Nb_2O_5 nanorods.

Acknowledgements

This work was partially supported by the Program of Excellent Team and Internationalization Foundation at Harbin Institute of Technology. C.Y.X. thanks financial support from Postdoctoral Science Foundation of Heilongjiang Province (LBH-Z08112) and China Postdoctoral Science Foundation (Nos. 20080440126, 200902381). The authors thank Prof. Zhong Lin Wang for his kind permission to use facilities at Georgia Institute of Technology.

References

[1] X. Li, N. Kikugawa, J. Ye, Nitrogen-doped lamellar niobic acid with visible light responsive photocatalytic activity, Adv. Mater. 20 (2008) 1–4.
[2] T. Iizuka, K. Ogasawara, K. Tanabe, Acidic and catalytic properties of niobium pentaoxide, Bull. Chem. Soc. Jpn. 56 (1983) 2927–2931.
[3] J. Yoshimura, Y. Ebina, J. Kondo, K. Domen, Visible light-induced photocatalytic behavior of a layered perovskite-type rubidium lead niobate, $RbPb_2Nb_3O_{10}$, J. Phys. Chem. 97 (1993) 1970–1973.
[4] L. Zhang, W. Zhang, L. Lu, X. Yang, X. Wang, Synthesis, structure and photocatalytic reactivity of layered CdS/$H_2La_2Ti_3O_{10}$ nanocomposites, J. Mater. Sci. 41 (2006) 3917–3921.
[5] K. Domen, Y. Ebina, T. Sekine, A. Tanakaa, J. Kondo, C. Hirose, Ion-exchangeable layered niobates as photocatalysts, Catal. Today 16 (1993) 479–486.
[6] G.B. Saupe, C.C. Waraksa, H.-N. Kim, Y.J. Han, D.M. Kaschak, D.M. Skinner, T.E. Mallouk, Nanoscale tubules formed by exfoliation of potassium hexaniobate, Chem. Mater. 12 (2000) 1556–1562.
[7] Y. Kobayashi, H. Hata, M. Salama, T.E. Mallouk, Scrolled sheet precursor route to niobium and tantalum oxide nanotubes, Nano Lett. 7 (2007) 2142–2145.
[8] A.R. Armstrong, G. Armstrong, J. Canales, P.G. Bruce, TiO_2-B nanowires, Angew. Chem. Int. Ed. 43 (2004) 2286–2288.
[9] T. Maruyama, S. Arai, Electrochromic properties of niobium oxide thin films prepared by radio-frequency magnetron sputtering method, Appl. Phys. Lett. 63 (1993) 869–870.
[10] M.E. Gimon-Kinsel, K.J. Balkus Jr., Pulsed laser deposition of mesoporous niobium oxide thin films and application as chemical sensors, Microporous Mesoporous Mater. 28 (1999) 113–123.
[11] F. Richter, H. Kupfer, P. Schlott, T. Gessner, C. Kaufamnn, Optical properties and mechanical stress in SiO_2/Nb_2O_5 multilayers, Thin Solid Films 389 (2001) 278–283.
[12] C.C. Lee, C.L. Tien, J.C. Hsu, Internal stress and optical properties of Nb_2O_5 thin films deposited by ion-beam sputtering, Appl. Opt. 41 (2002) 2043–2047.
[13] C.M. Lieber, Z.L. Wang, Functional nanowires, MRS Bull. 32 (2007) 99–108.
[14] J. Liu, H. Xia, L. Lu, D.F. Xue, Anisotropic Co_3O_4 porous nanocapsules toward high-capacity Li-ion batteries, J. Mater. Chem. 20 (2010) 1506–1510.
[15] M.N. Liu, D.F. Xue, Amine-assisted route to fabricate $LiNbO_3$ particles with a tunable shape, J. Phys. Chem. C 112 (2008) 6346–6351.
[16] M. Mozetič, U. Cvelbar, M.K. Sunkara, S. Vaddiraju, A method for the rapid synthesis of large quantities of metal oxide nanowires at low temperatures, Adv. Mater. 17 (2005) 2138–2142.
[17] B. Varghese, S.C. Haur, C.T. Lim, Nb_2O_5 nanowires as efficient electron field emitters, J. Phys. Chem. C 112 (2008) 10008–10012.
[18] M.D. Wei, Z.M. Qi, M. Ichihara, H.S. Zhou, Synthesis of single-crystal niobium pentoxide nanobelts, Acta Mater. 56 (2008) 2488–2494.
[19] C.L. Yan, D.F. Xue, Formation of Nb_2O_5 nanotube arrays through phase transformation, Adv. Mater. 20 (2008) 1055–1058.
[20] C.L. Yan, J. Liu, F. Liu, J.S. Wu, K. Gao, D.F. Xue, Tube formation in nanoscale materials, Nanoscale Res. Lett. 3 (2008) 473–480.
[21] F. Liu, D.F. Xue, Controlled fabrication of Nb_2O_5 hollow nanospheres and nanotubes, Mod. Phys. Lett. 23 (2009) 3769–3775.
[22] F. Liu, D.F. Xue, One-step solution-based strategy to 3D superstructures of Nb_2O_5–LiF, Nanosci. Nanotechnol. Lett. 1 (2009) 66–71.
[23] M.N. Liu, D.F. Xue, Large-scale fabrication of $H_2(H_2O)Nb_2O_6$ and Nb_2O_5 hollow microspheres, Mater. Res. Bull. 45 (2010) 333–338.
[24] J. Liu, D.F. Xue, Thermal oxidation strategy towards porous metal oxide hollow architectures, Adv. Mater. 20 (2008) 2622–2627.
[25] C.Y. Xu, L. Zhen, R.S. Yang, Z.L. Wang, Synthesis of single-crystalline niobate nanorods via ion-exchange based on molten-salt reaction, J. Am. Chem. Soc. 129 (2007) 15444–15445.
[26] V.K. Kato, S. Tamura, Die kristallstruktur von T-Nb_2O_5, Acta Crystallogr. B 31 (1975) 673–677.